

## String potential model: Spinless quarks

Dan LaCourse and M. G. Olsson

*Physics Department, University of Wisconsin, Madison, Wisconsin 53706*

(Received 26 September 1988)

We propose a generalization of the usual potential model of quark bound states in which the confining flux tube is a dynamical object carrying both angular momentum and energy. The  $Q\bar{Q}$ -string system with spinless quarks is quantized using an implicit operator technique and the resulting relativistic wave equation is solved. For heavy quarks the usual Schrödinger valence-quark model is recovered. The Regge slope with light quarks agrees with the classical rotating-string result and is significantly larger than that given by the normal potential model. Quark mass variation and the effects of short-range forces are also considered.

### I. INTRODUCTION

The basic problem of hadron dynamics is to understand the properties of hadron states from first principles. Although the theory of quark-gluon dynamics is widely accepted we are still far from such a fundamental explanation especially for states containing light quarks. In the case of heavy-quark bound states the nonrelativistic potential<sup>1</sup> model has had numerous impressive successes in the calculation of masses, annihilation rates, and electromagnetic transitions. For light quarks the potential model also works well but it is no longer clear that the confining interaction should be a static potential or even what its Lorentz nature should be.

Much effort<sup>1,2</sup> has gone into the generalization of the nonrelativistic potential model. If one ignores quark spin effects the most straightforward procedure is to replace the nonrelativistic energy by the relativistic expression giving the wave equation

$$[2\sqrt{p^2 + m^2} + V(r) - M]\psi(r) = 0. \quad (1)$$

For simplicity we consider here only equal-mass quarks. The above equation is known as the "square root" equation or the "spinless Salpeter" equation. The spinless Salpeter equation is reasonably successful from a phenomenological point of view in explaining spin-averaged heavy-quarkonia data.<sup>3</sup>

The major justification of the potential model for large quark separations lies in the hadronic string model first proposed by Nambu.<sup>4</sup> In this picture the quarks are connected by a stringlike color flux tube which naturally yields a linear confinement potential. The spin dependence of the quark-quark interaction at large distances consists of the kinematic Thomas spin-orbit term alone.<sup>5</sup> This is consistent with QCD in the quenched low-velocity approximation.<sup>6</sup>

The string model also makes<sup>4</sup> a striking prediction for the Regge slope:

$$\alpha' = (2\pi a)^{-1}, \quad (2)$$

where  $\alpha' = dJ/dM^2$  and  $J$  is the angular momentum,  $M$  is the state mass, and  $a$  is the string tension. This result fol-

lows for a rotating classical string with massless quarks. The dynamic string model thus differs conceptually from the valence potential model in that the string can carry both angular momentum and energy. Our aim in this paper is to unify the potential and string models, at least for spinless quarks. This will entail quantization of the quark-string system.

We will often be comparing our string-potential model with spinless Salpeter equation results. As a benchmark we plot in Fig. 1 the leading and daughter Regge trajectories for the spinless Salpeter equation (1) for massless quarks and a linear confinement potential

$$m = 0, \quad V(r) = ar, \quad a = 0.2 \text{ GeV}^2. \quad (3a)$$

We note that linear confinement yields straight line Chew-Frautschi plots. Two aspects of this plot are noteworthy: (i) The slope of the trajectory is  $0.64 \text{ GeV}^{-2}$  whereas the string model slope of Eq. (2) gives

$$\alpha' = (2\pi a)^{-1} \simeq 0.80 \text{ GeV}^{-2}, \quad (3b)$$

for the same string tension  $a = 0.2 \text{ GeV}^2$ ; (ii) the intercept  $\alpha(0)$  is negative, whereas known leading meson Regge trajectories have a positive intercept. The discrepancy in slope between the potential and string models is the primary question which we attempt to resolve here. Our synthesized string-potential model for spinless quarks reduces to Eq. (1) when  $J=0$  and yields a very similar Regge trajectory to the classical string model with quarks on its ends. The slope is quite insensitive to the quark mass (as long as  $m \lesssim 0.25 \text{ GeV}$ ) and also to short-range potentials added to the confining part. We believe that the intercept depends critically on the spin of the quarks. The intercept question will be discussed in more detail at the end of this paper.

Our principal assumption is that the string always lies in a straight line between the quarks. The quarks move freely so that both rotation and radial motion can occur. The entire system is quantized in orbital angular momentum and energy. Since the string appears in the Hamiltonian its angular momentum and energy combined with the quarks form a single quantum system.

The two eigenstate equations (energy and angular

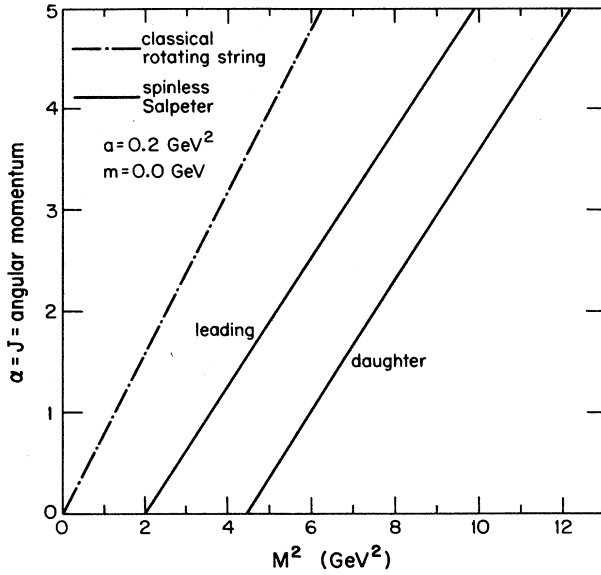


FIG. 1. Chew-Frautschi plot comparing the classical rotating string and the spinless Salpeter prediction with linear confinement and massless quarks. The string tension is the same in both cases.

momentum) involve transcendental functions of a common operator, the quark transverse velocity  $v_{\perp}$ . The presence of this operator makes the quantum-mechanical solution technically difficult. We proceed by expanding the states in a truncated series

$$\psi(\mathbf{r}) = \sum_{i=1}^N c_i e_i(\mathbf{r}), \quad (4)$$

where  $\{e_i(\mathbf{r})\}$  form a convenient complete set.<sup>3</sup> The operators are expanded in a corresponding manner. The eigenvalue equations now become finite matrix equations. The angular momentum matrix equation can be used to find the  $v_{\perp}$  matrix which then is substituted into the energy eigenvalue equation. A potential problem is that  $v_{\perp}$  occurs in transcendental forms whose matrix elements are difficult to calculate directly. We instead perform these functions on the  $v_{\perp}$  matrix by rotating to a basis set where  $v_{\perp}$  is diagonal, operating on the diagonal elements, and rotating back.

The plan of the paper is to first discuss the classical canonical string model in Sec. II. The quantized version and its limiting cases are given in Sec. III. Sec. IV contains some of the details involved in the quantum solution and our results and a discussion are found in Sec. V.

## II. CLASSICAL STRAIGHT-STRING MOTION

We begin by reviewing the classical motion<sup>7</sup> of a quark pair at the ends of a straight string. Since the system is central we can, without loss of generality, consider the system to be moving in a plane as shown in Fig. 2. The coordinate  $\mathbf{r}_i$  denotes the  $i$ th quark's position from the center of momentum which is assumed stationary. The relativistic Lagrangian for the  $i$ th quark and the portion

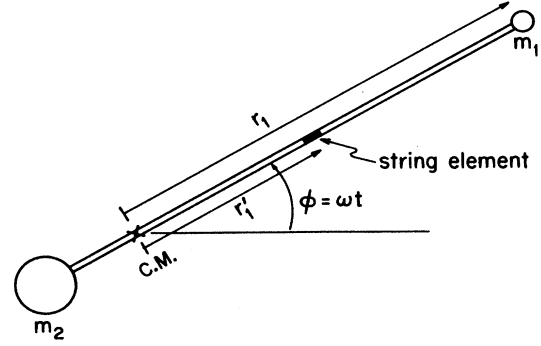


FIG. 2. Geometry of the string-potential model.

of string from the c.m. to the quark is

$$L_i = -m_i(1-v_i^2)^{1/2} - a \int_0^{r_i} dr'_i [1-(v'_{i\perp})^2]^{1/2}, \quad (5)$$

where  $v'_{i\perp}$  is the transverse velocity of a string element at distance  $r'_i$  and is related to  $r'_i$  in terms of the angular velocity  $\omega$  as

$$v'_{i\perp} \equiv \omega r'_i. \quad (6)$$

The quark's speed  $v_i$  is given by

$$v_i^2 = \dot{r}_i^2 + v_{i\perp}^2. \quad (7)$$

The partial canonical momenta are then

$$p_{ir} = \frac{\partial L_i}{\partial \dot{r}_i} = m_i \dot{r}_i \gamma_i, \quad (8)$$

$$p_{i\phi} = \frac{\partial L_i}{\partial \omega} = m_i r_i^2 \omega \gamma_i + a \omega \int_0^{r_i} dr'_i (r'_i)^2 \gamma'_{i\perp}, \quad (9)$$

where  $\gamma_i^{-2} = 1 - v_i^2$  and  $(\gamma'_{i\perp})^{-2} = 1 - (v'_{i\perp})^2$ . The Hamiltonian for the  $i$ th part of the system is found from the above to be

$$H_i = \dot{r}_i p_{ir} + \omega p_{i\phi} - L_i = m_i \gamma_i + a \int_0^{r_i} dr'_i \gamma'_{i\perp}. \quad (10)$$

The physical interpretation of Eqs. (9) and (10) is quite clear. The first term represents the quark angular momentum and energy, respectively; and the second terms are the corresponding quantities for the string portion.

By explicit integration Eqs. (9) and (10) become

$$J_i \equiv p_{i\phi} = m_i r_i v_{i\perp} \gamma_i + 2a r_i^2 f_i, \quad (11)$$

$$4v_{i\perp} f_i = \frac{\arcsin v_{i\perp}}{v_{i\perp}} - (1 - v_{i\perp}^2)^{1/2},$$

and

$$H_i = m_i \gamma_i + a r_i \frac{\arcsin v_{i\perp}}{v_{i\perp}}. \quad (12)$$

The procedure normally would be to use Eqs. (8) and (11) to eliminate  $\dot{r}$  and  $\omega$  in favor of the canonical momenta. For this system only  $\dot{r}$  can be explicitly eliminated. From Eq. (8) we obtain

$$\dot{r}_i^2 = \frac{p_{ir}^2}{p_{ir}^2 + m_i^2} (1 - v_{i\perp}^2)$$

and hence

$$m_i \gamma_i = W_{ir} \gamma_{i\perp}, \quad (13)$$

where

$$W_{ir} \equiv (p_{ir}^2 + m_i^2)^{1/2}. \quad (14)$$

Using Eq. (13) in Eqs. (11) and (12) we find

$$J_i = r_i v_{i\perp} \gamma_{i\perp} W_{ir} + 2ar^2 f_i, \quad (15)$$

$$H_i = \gamma_{i\perp} W_{ir} + ar_i \frac{\arcsin v_{i\perp}}{v_{i\perp}}. \quad (16)$$

For simplicity we concentrate on the equal quark mass case ( $m_1 = m_2$ ) so that  $H = H_1 + H_2 = 2H_1$  and  $J = J_1 + J_2 = 2J_1$ . For the remainder of this paper it is understood that  $v_\perp \equiv v_{1\perp}$ ,  $\gamma_{1\perp} \equiv \gamma_\perp$  and the interquark distance  $r = 2r_1$ . Equations (15) and (16) then become

$$J = rv_\perp \gamma_\perp W_r + ar^2 f(v_\perp), \quad (17)$$

$$H = 2\gamma_\perp W_r + ar \frac{\arcsin v_\perp}{v_\perp}, \quad (18)$$

where<sup>8</sup>  $W_r \equiv (p_r^2 + m^2)^{1/2}$  and

$$4v_\perp f(v_\perp) \equiv \frac{\arcsin v_\perp}{v_\perp} - (1 - v_\perp^2)^{1/2}.$$

A useful classical limit is the case of massless quarks moving in circular orbits. Lagrange's equation for  $r_1$  in the circular orbit limit gives

$$a(1 - \omega^2 r_1^2) = m\omega^2 r_1,$$

which when combined with Eqs. (17) and (18) shows that the quarks do not carry momentum in the  $m = 0$  limit. In this limit  $\gamma_\perp W_r = 0$  and  $v_\perp = 1$  so Eqs. (17) and (18) become

$$J = \frac{ar^2\pi}{8}, \quad H \equiv M = \frac{ar\pi}{2}.$$

Elimination of  $r$  gives

$$J = \frac{1}{2\pi a} M^2, \quad (19)$$

yielding the Regge slope

$$\alpha' \equiv \frac{dJ}{dM^2} = \frac{1}{2\pi a}. \quad (20)$$

### III. QUANTIZATION AND LIMITING BEHAVIOR

In principle the classical string model Eqs. (17) and (18) are quantized by the replacements<sup>8</sup>

$$J \rightarrow \sqrt{l(l+1)}, \quad p_r^2 \rightarrow -\frac{1}{r} \frac{\partial^2}{\partial r^2} r. \quad (21)$$

The angular momentum quantization condition follows from the rotational invariance of the system. Of course

the quantities  $r$ ,  $H$ , and  $v_\perp$  must now be treated as operators.

The dynamical quantities  $r$ ,  $H$ , and  $v_\perp$  are regarded as Hermitian noncommuting operators. This is inconsistent with Eqs. (17) and (18) unless the equations are symmetrized as

$$\frac{2\sqrt{l(l+1)}}{r} = \{v_\perp \gamma_\perp, W_r\} + a\{r, f(v_\perp)\}, \quad (22)$$

$$H = \{\gamma_\perp, W_r\} + \frac{a}{2} \left\{ r, \frac{\arcsin v_\perp}{v_\perp} \right\}, \quad (23)$$

$$HR(r) = MR(r). \quad (24)$$

The state function is  $\psi(\mathbf{r}) = R(r)Y_l^m(\theta, \phi)$  and  $\{A, B\} \equiv AB + BA$ .

Before we attempt a general solution it is profitable to discuss some examples of limiting behavior.

#### A. Nonrelativistic limit

In the nonrelativistic heavy-quark limit we expect that  $p_r^2 \ll m^2$ ,  $v_\perp \ll 1$ , and  $ar \ll m$ . To leading order Eqs. (22) and (23) become

$$v_\perp \simeq \frac{\sqrt{l(l+1)}}{mr}, \quad (25)$$

$$H \simeq 2m \left[ 1 + \frac{p_r^2}{2m^2} \right] \left[ 1 + \frac{v_\perp^2}{2} \right] + ar,$$

or, by elimination of  $v_\perp$ ,

$$H \simeq 2m + \frac{1}{m} \left[ p_r^2 + \frac{l(l+1)}{r^2} \right] + ar. \quad (26)$$

This is the standard Schrödinger valence-quark potential model with linear confinement. The Schrödinger limit clearly illustrates that the  $ar(\arcsin v_\perp)/v_\perp$  term in the quark-string model contains the normal static linear confinement. For massive slowly moving quarks the string carries a negligible fraction of the kinetic energy and angular momentum and the standard valence-quark model reappears.

#### B. Zero angular momentum

When  $l = 0$  Eq. (22) implies that  $v_\perp = 0$  and when this is substituted back into Eq. (23) the Hamiltonian becomes

$$H = 2(p_r^2 + m^2)^{1/2} + ar, \quad (27)$$

which is the spinless Salpeter equation for zero angular momentum. This might be expected since for radial quark motion the string has no kinetic energy. Again the valence-quark potential model is recovered, this time for relativistic motion.

As we have seen in this section the coupled Eqs. (22)–(24) reduce in various limits to potential models with a linearly confining potential. An obvious and useful generalization is to add a short-range potential  $V_S(r)$  to represent  $Q\bar{Q}$  interactions other than the confining part. The final result is

$$\frac{2\sqrt{l(l+1)}}{r} = \{v_\perp \gamma_\perp, W_r\} + a \{r, f(v_\perp)\}, \quad (28)$$

$$H = \{\gamma_\perp, W_r\} + \frac{a}{2} \left\{ r, \frac{\arcsin v_\perp}{v_\perp} \right\} + V_S(r), \quad (29)$$

$$HR(r) = MR(r),$$

where the state function  $\psi(\mathbf{r}) = R(r)Y_l^m(\theta, \phi)$  and

$$W_r = (p_r^2 + m^2)^{1/2}, \quad (30)$$

$$4v_\perp f(v_\perp) = \frac{\arcsin v_\perp}{v_\perp} - (1 - v_\perp^2)^{1/2},$$

and  $\gamma_\perp = (1 - v_\perp^2)^{-1/2}$ ,  $\{A, B\} = AB + BA$ .

#### IV. SOLVING THE QUANTIZED STRING-POTENTIAL EQUATIONS

The system of operator Eqs. (28)–(30) form a mathematical statement of the problem we wish to solve. Ideally it would be best to eliminate the operator  $v_\perp$  using Eq. (28) and then to solve the resulting radial-type equation. Since this goal is clearly impossible we must develop a numerical scheme to effectively carry this out. Complicating matters further, the various functions of  $v_\perp$  in Eqs. (28) and (29) are related only transcendently. This means that the elements of one matrix function of  $v_\perp$  are not simply related to the elements of another function of  $v_\perp$ .

One can think of the angular momentum Eq. (28) as a sort of eigenvalue equation for  $v_\perp$ . When  $v_\perp$  is diagonalized the problem of relating different functions of  $v_\perp$  is vastly simplified. Our approach is to approximate the wave function as in Eq. (4) by a finite set of basis states.<sup>3</sup> Equations (28) and (29) then become finite matrix equations.

The solution procedure is then, for a given  $N$  basis set approximation: (i) Assume a set of  $\frac{1}{2}N(N+1)$  symmetric  $v_\perp$  elements; (ii) diagonalize  $v_\perp$  to obtain the  $N$  eigenvalues; (iii) in this diagonal representation compute  $f(v_\perp)$  and  $\gamma(v_\perp)$  then rotate back to obtain these matrices in the original basis representation; (iv) vary the elements of  $v_\perp$  to best satisfy Eq. (28); (v) substitute the resulting  $v_\perp$  solution into Eq. (29) and solve as a standard eigenvalue problem for the eigenstate mass  $M$ .

The above procedure works efficiently to obtain the state mass  $M$ . We have found that an excellent set of starting elements for step (i) is obtained by ignoring the operator symmetrizations in Eq. (28). We represent  $v_\perp$  as  $VDV^{-1}$  where  $V$  is a rotation matrix and  $D$  is a diagonal matrix containing the  $v_\perp$  eigenvalues, and for the unsymmetrized case  $V^{-1} \neq V^T$ . The unsymmetrized equation can then be solved directly as a nearly standard eigenvalue equation for  $v_\perp$ . As might be expected the  $v_\perp$  matrix in the unsymmetrized case is not symmetric but the averaged elements are not far from the final  $v_\perp$  elements. In all cases we have encountered, only a few iterations are needed to achieve the symmetrized solution.

The convergence to a stable solution is quite rapid in terms of the number of basis states needed. For zero

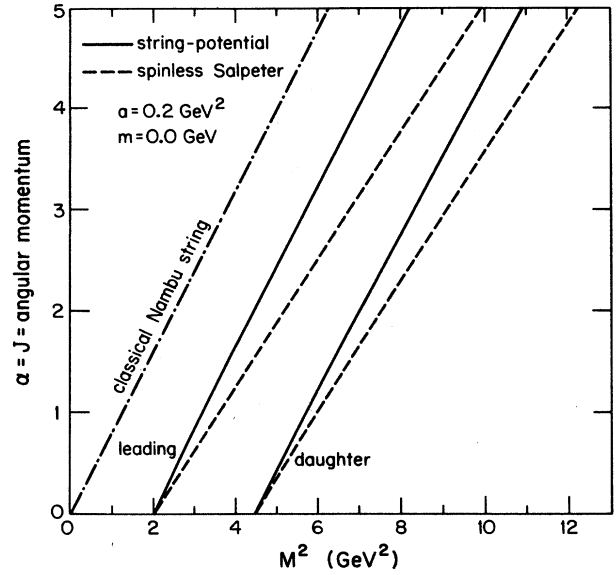


FIG. 3. Chew-Frautschi plot of the quantized string-potential leading and first-daughter trajectories for zero-mass quarks. For comparison we include the classical rotating string and spinless Salpeter results.

mass quarks the lowest two radial states are determined to 10 MeV with five basis states and 1 MeV with ten basis states. The most difficult aspect is the initial computation of the  $W_r$  operator. This square-root operator is computed by first evaluating  $\langle p_r^2 \rangle$ , diagonalizing and taking the positive square root  $(p_r^2 + m^2)^{1/2}$  of the eigenvalues. The square-root operator is then rotated back to the original basis set. The result converges rapidly for  $l=0$ , but only slowly for  $l>0$ .

The results are shown in Fig. 3 for massless quarks for the leading and daughter trajectories. We see that the slope of the trajectory is close to the classical Nambu string slope while the  $J=0$  intercept is the same as the spinless Salpeter result with linear confinement. For a string tension of  $a=0.2 \text{ GeV}^2$  we find the Regge slope for the quantized string-potential model is  $0.79 \text{ GeV}^{-2}$  whereas the classical rotating string has  $\alpha' \simeq 0.80 \text{ GeV}^{-2}$ . Note that the two models differ physically in that ours allows radial motion, while the Nambu string does not. As seen in Fig. 3 the effect of radial motion and quantization changes the intercept but leaves the slope essentially unchanged.

#### V. DISCUSSION

We have developed here a quantized version of the string-potential model for the case of zero spin quarks. The new feature of this model is that the string and quarks share in carrying energy and angular momentum. Technically, we have developed a new technique to numerically handle an implicit operator present when canonical quantization of the system is attempted.

In our model the quarks at the ends of a straight string

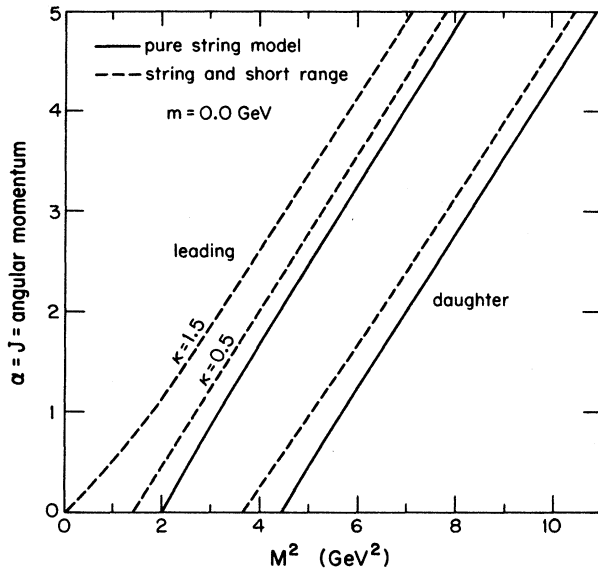


FIG. 4. Quantum string-potential model with  $m = 0$  showing the leading and daughter (first radial excitation) trajectories. The dashed curves show the effect of the short-range Coulombic interaction of Eqs. (31) with  $\kappa = 0.5$  and  $\kappa = 1.5$ .

can move radially or rotationally. The string has potential stretch energy but only rotational kinetic energy. For very heavy quarks the quarks carry most of the angular momentum and kinetic energy so the string effectively acts as a linearly confining static potential. For relativistic motion we feel that this approach represents the most physically motivated generalization of the potential model.

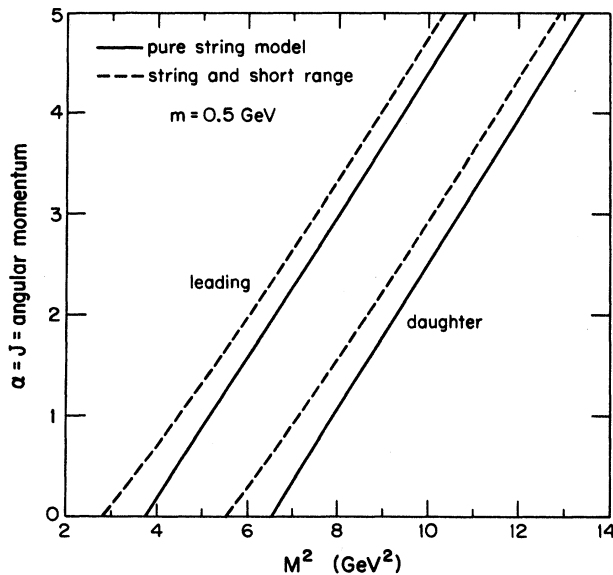


FIG. 5. Same as Fig. 4 but with quark mass  $m = 0.5$  GeV. The insensitivity of the state mass to small quark masses can be seen by comparing to Fig. 4.

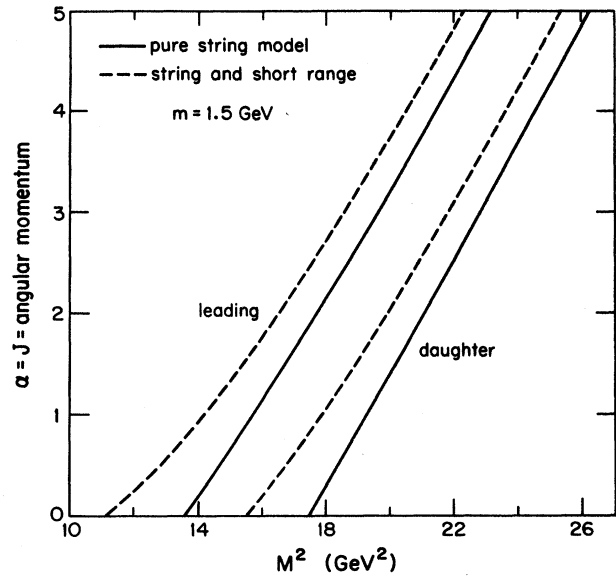


FIG. 6. Same as Fig. 4 but with  $m = 1.5$  GeV.

For light quarks the quantized string model is qualitatively similar to the classical rotating string except that the  $J = 0$  intercept is positive. This positivity is a direct result of the radial quark motion and the solution of the spinless Salpeter equation. The Regge slope is  $0.79 \text{ GeV}^{-2}$  which is virtually identical to the Nambu string slope of  $0.80 \text{ GeV}^{-2}$  as given in Eqs. (3) with a normal string tension  $a = 0.20 \text{ GeV}^2$ . These trajectory slopes might be compared with  $\alpha' = 0.64 \text{ GeV}^{-2}$  from the pure relativistic potential model with the same string tension as shown in Fig. 3.

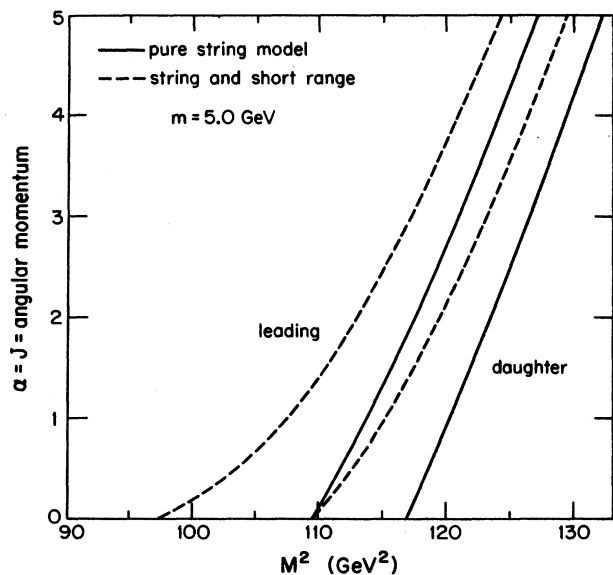


FIG. 7. Same as Fig. 4 but with  $m = 5$  GeV. For heavy-quark states the short-range interaction has a larger effect.

For larger quark masses we find an increase in intercept and a decrease in slope of the Chew-Frautschi plot. Figures 4–7 depict the leading trajectory and first daughter trajectory for quark masses of 0, 0.5, 1.5, and 5 GeV, respectively. The solid curves represent the pure string-potential model with no short-range component. Increasing the quark mass from zero to 0.25 GeV has only a minimal effect on the trajectory. This observation is consistent with the universal slope behavior of all light meson and baryon states.<sup>9</sup> For heavy-quark masses the slope decreases significantly for low angular momentum. When the state mass is much larger than the quark mass the slope will reduce to the massless quark value. The intercept value reflects the rest mass of the quarks.

We next consider the addition of a short-distance interaction of the Cornell type:

$$V_S(r) = \frac{-\kappa}{r}, \quad (31)$$

where normally  $\kappa \simeq 0.5$ . The results are shown by the dashed curves of Figs. 4–7. We observe that this short-distance potential has the least effect on light-quark-mass dynamics. This might be expected since light-quark states are larger than those with heavy quarks and hence less sensitive to short-range interactions. While it is possible to significantly reduce the intercept for large  $\kappa$  ( $\kappa = 1.5$ ), the linearity of the trajectory is lost. The  $m = 1.5$  and 5 GeV trajectories are significantly changed by the  $\kappa = 0.5$  short-range term, especially for small angular momentum.

Normal leading meson Regge trajectories have negative  $J=0$  intercepts.<sup>9</sup> The intercept in our model is positive and is exactly equal to the ground-state solution to the spinless Salpeter Eq. (1) for zero angular momentum. The intercept value is only weakly dependent on quark mass variations up to 0.25 GeV or to the presence of short-range forces of the type in Eq. (31). The difference lies in the neglect of quark spin since two spin- $\frac{1}{2}$  quarks in a spin-triplet state will shift the Regge trajectory upward by one unit.

In order to more directly compare our spinless model to experimental data we have constructed a *spin-averaged* Regge trajectory using light isospin one mesons. The zero orbital angular momentum spin-averaged state is formed in the usual manner from the  $\rho$  and  $\pi$  states and the  $l=1$  state from the  $a_0$ ,  $a_1$ ,  $a_2$ , and  $b_1$  meson states. These values, shown in Fig. 8, define a spin-averaged leading meson trajectory having the same slope as the

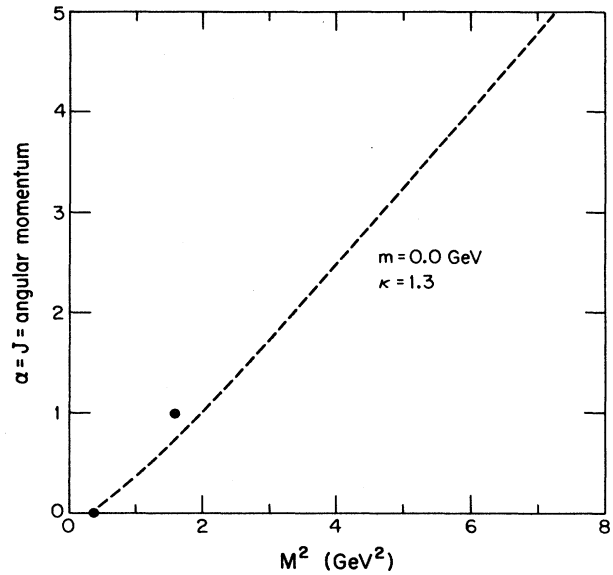


FIG. 8. Experimental spin-averaged isospin one-meson trajectory. The dashed curve is the string-potential trajectory with a short-range force given by Eq. (31) with  $\kappa = 1.3$ .

Nambu string. For comparison we show the  $m=0$  trajectory of our string-potential model with a  $\kappa=1.3$  short-range interaction. While the spin-averaged intercept is now positive the predicted trajectory does not pass through both points since the short-range interaction causes a curvature in the trajectory.

It is evident that we have not yet achieved a phenomenologically complete description of meson systems. This is most clearly seen in the above discussion of the intercept problem. We believe though that the potential-string model has a strong physical motivation and is worth additional effort to achieve a more realistic picture.

#### ACKNOWLEDGMENTS

We are grateful to Manuel Drees, Xerxes Tata, C. J. Suchyta, and Robert Fletcher for interesting discussions. This research was supported in part by the University of Wisconsin Research Committee with funds granted by the Wisconsin Alumni Research Foundation, and in part by the U.S. Department of Energy under Contracts Nos. DE-AC02-76ER00881 and DE-FG02-84ER40173.

<sup>1</sup>T. Appelquist, R. M. Barnett, and K. D. Lane, *Annu. Rev. Nucl. Part. Sci.* **28**, 387 (1978); V. A. Novikov, L. B. Okun, M. A. Shifman, A. I. Vainshtein, M. B. Voloshin, and V. I. Zakharov, *Phys. Rep.* **41C**, 1 (1978); C. Quigg and J. L. Rosner, *Phys. Rep.* **56**, 167 (1979); W. Buchmüller, *Fundamental Interactions in Low-Energy Systems*, edited by P. Dapiatz, G. Fiorentini, and G. Torelli (Plenum, New York, 1985); J. L. Rosner, in *Quantum Gravity and Cosmology*, proceedings of the Eighth Kyoto Summer Institute, Kyoto, Japan, 1985, edited by H. Sato and T. Inami (World Scientific, Singapore,

1986); D. B. Lichtenberg, *Int. J. Mod. Phys. A* **2**, 1669 (1987).

<sup>2</sup>S. Godfrey and N. Isgur, *Phys. Rev. D* **32**, 189 (1985).

<sup>3</sup>S. Jacobs, M. G. Olsson, and C. J. Suchyta III, *Phys. Rev. D* **33**, 3338 (1986).

<sup>4</sup>For the development of the string model see, for instance, the following review articles: C. Rebbi, *Phys. Rep.* **12C**, 1 (1974); S. Mandelstam, *ibid.* **13C**, 259 (1974); T. Gotō, *Prog. Theor. Phys.* **46**, 1560 (1971); X. Artru, *Phys. Rep.* **97**, 147 (1983).

<sup>5</sup>W. Buchmüller, *Phys. Lett.* **112B**, 479 (1982).

<sup>6</sup>E. Eichten and F. L. Feinberg, *Phys. Rev. Lett.* **43**, 1205 (1979);

- Phys. Rev. D **23**, 2724 (1981); D. Gromes, Z. Phys. C **26**, 401 (1984).
- <sup>7</sup>M. Ida, Prog. Theor. Phys. **59**, 1661 (1978); A. Chodos and C. B. Thorn, Nucl. Phys. **B72**, 509 (1974); I. Bars, *ibid.* **B111**, 413 (1976).
- <sup>8</sup>Note that  $p_{1r} = \partial L_1 / \partial \dot{r}_1 = \partial(2L_1) / \partial(2\dot{r}_1) = \partial L / \partial \dot{r} = p_r$ .
- <sup>9</sup>V. Barger and D. Cline, *Phenomenological Theories of High Energy Scattering* (Benjamin, New York, 1969).